Microlithography

DOI: 10.1002/smll.200700881

A One-Step Route to a Perfectly Ordered Wafer-Scale Microbowl Array for Size-Dependent Superhydrophobicity **

*Xing-Jiu Huang, Joo-Hyung Lee, Jong-Won Lee, Jun-Bo Yoon, and Yang-Kyu Choi**

A superhydrophobic surface results from an increase in surface roughness.[1,2] Generally, regular rough surfaces have been fabricated. These not only exhibit remarkable superhydrophobic behavior,[3–8] but also are very useful for quantitative studies of the equilibrium configurations of droplets on rough substrates.[9] However, most of this research has been focused on structures of similar types, that is, those with so-called posts or pillars.[8,10–16] The main reason for this focus is the difficulties related to fabrication (for example, the need for complicated processes and expensive materials). These drawbacks restrict the development of a perfectly ordered rough surface and associated hydrophobic properties. Although an antifogging surface of arrayed micro-hemispheres has been fabricated, the procedure is complex.[17] Here, we introduce an easy, inexpensive, high-throughput, and scalable one-step microlithography, without the introduction of a nanostructure, that can be used in combination with microstructures to make hydrophobic surfaces. The proposed structure was composed of a wafer-scale, perfectly ordered, microbowl array. The surface was precisely designed with specific dimensions and then the hydrophobic behavior depending on these dimensions was investigated analytically and modeled. The apparent contact angle, θ_{app}, was dependent on the ratio of diameter to height ($2d/h$) in the microbowl. This paper also suggests how a highly superhydrophobic surface should be designed to avoid a transition between hydrophobicity and hydrophilicity. In the longer term, the microbowl-arrayed surface may lead to new important applications for many industrial processes, such as in high-speed submarines, ships, and aircraft, as well as antifog materials for eye glasses, swimming goggles, or antifog glass for the windshield of cars, and so on.

The fabrication process of a photoresist microbowl array with three-dimensional diffuser lithography [18,19] that used randomized ultraviolet (UV) light is schematically shown in Figure 1. For further details about the fabrication process, see the Experimental Section. A typical low-magnification scanning electron microscopy (SEM) image (Figure 2a) shows that a highly uniform surface with few defects was obtained by the one-step method presented. A sequence of photographs of a droplet lowered onto the surface was recorded to probe the hydrophobic behavior (Figure 2b). In this sequence a clear comparison of droplet shape is displayed for the initial state due to the gravity; the exact contacting state; the tight and severe contacting states under pressure; the state when removed from the array substrate. When the droplet just touched the surface, it did not change from its initial shape. A similar phenomenon was observed when the droplet is in tight or severe contact with the surface; when the array substrate was removed from the droplet, no remaining water was observed. This observation verified the existence of a superhydrophobic surface in which the vertical adhesive force between the sample and the droplet was extremely feeble and could be ignored.[20] To explore the effects of the geometry of such a perfectly ordered microbowl surface on the wetting behavior, we compared the contact angle (θ) of a droplet on a flat surface and microbowl array surface before and after silane modification (Figure 2c). Clearly, a flat or microbowl-arrayed surface

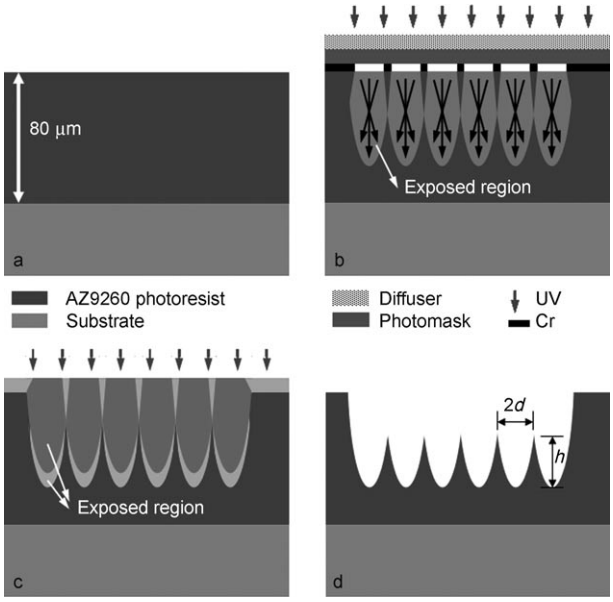

Figure 1. Fabrication process of the Cassie–Baxter microbowl array. a) An 80-μm positive photoresist spin-coated on a silicon substrate. b) UV exposure of the photoresist through a diffuser and photomask. c) UV flood exposure. d) A fabricated Cassie–Baxter photoresist microbowl array after development ($2d$ is the diameter in μm, h is the height in μm).

[*] Dr. X.-J. Huang, J.-W. Lee, Prof. Y.-K. Choi
Nano-Oriented Bio-Electronic Lab
School of Electrical Engineering and Computer Science
Korea Advanced Institute of Science and Technology
Daejeon, 305-701 (South Korea)
Fax: (+82) 505-869-347-7
E-mail: ykchoi@ee.kaist.ac.kr
J.-H. Lee, Prof. J.-B. Yoon
3D Micro-Nano Structures Lab
School of Electrical Engineering and Computer Science
Korea Advanced Institute of Science and Technology
Daejeon, 305-701, (South Korea)

[**] Dr. X.-J. Huang would like to express appreciation for the financial support of the Brain Korea 21 project, the school of Information Technology, and the Korea Advanced Institute of Science and Technology in 2007. Also this work was partially supported by the NRL program of the Korea Science and Engineering Foundation grant funded by the Korea government (MOST) (No.RoA-2007-000-20028-0).

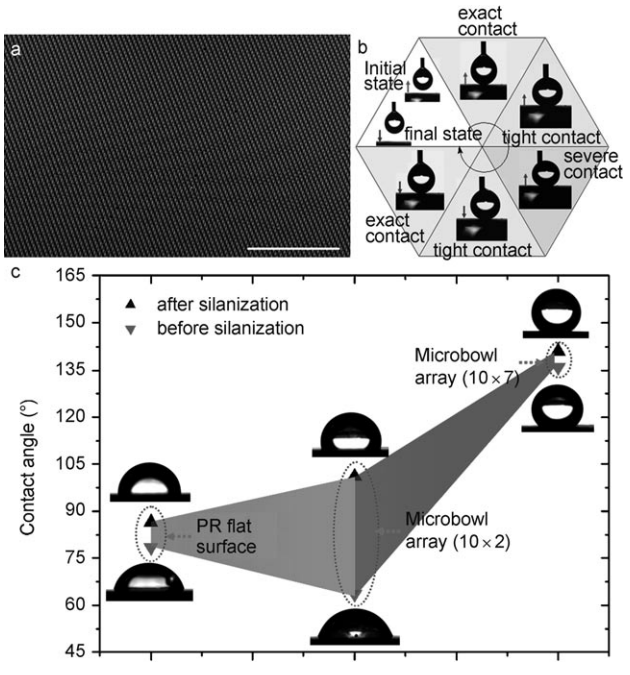

Figure 2. Highly uniform array and corresponding hydrophobic behaviour. a) A low-magnification SEM image of a Cassie–Baxter microbowl array (30×30). The scale bar is 500 μm. b) Sequential photographs in the droplet to be downed were recorded before and after the water droplet made contact with the silane-modified microbowl array of 10×18. c) The comparison between the wetting behavior of a flat surface and the Cassie–Baxter microbowl array (10×2, 10×7) surface before and after silanization.

with lower surface energy could be created that had an increased contact angle because of close packing of trifluoromethyl groups (-CF_3).[21,22] When the flat surface was changed to a 10×2 ($2d \times h$ in μm unless otherwise stated) microbowl array before silanization, θ decreased from 78.5° to 63.5° because of the increased surface roughness[4] (both hydrophobicity and hydrophilicity are reinforced by roughness[23]), which resulted in geometrical enhancement of the hydrophilicity. The arrayed-microbowls acted as reservoirs that aided fast spreading of the liquid front,[23] the liquid accumulated within the corrugation,[9] and spread much faster than on the flat surface.[24] A 10×2 microbowl array with packed -CF_3 groups displayed better hydrophobic behavior (θ = 101°) because of the lower surface energy, whereas the contact angle for a corresponding flat surface was about 86.5°. Obviously, such a microbowl-arrayed structure had a significant effect on antiwetting behavior. Interestingly, when the height of the microbowls was increased from 10×2 to 10×7, the surface exhibited much better hydrophobicity; θ actually reached 136° without silane modification. It was significant that this situation could not be ascribed to surface roughness, but was mainly rationalized considering trapped air below the droplet (Cassie–Baxter model[25]). Further confirmation was found by looking at the contact angle of a 10×7 microbowl array surface before and after silanization. We observed that θ only reached 141° after silanization, suggesting that the geometrical effect was dominant in this case ($\Delta\theta_{10\times7} < \Delta\theta_{10\times2}$, where $\Delta\theta$ is the difference in θ after and before silanization). From this experiment, we concluded that such a perfectly ordered microbowl array geometrically and crucially influences the hydrophobic behavior of the surfaces.

What should the parameters of this unique geometry be for it to result in a superhydrophobic surface? To answer this question, we compared several previously reported models [10,12,13,25]. This led us to suggest the following theoretical model of our microbowl array for the quantitative prediction of apparent contact angles (Figure 3). We could clearly observe the changes in geometric parameters from the comparison of the cross-sectional views of square pillars, cylindrical asperities or posts and hemispherical-top pillars, and the microbowl array (Figure 3). In particular, the microbowl array had a parabolic curvature, the post- or pillar-tops change to very sharp peaks (Figure 3b, inset). When reduced to the most basic shape units of square pillars, cylindrical asperities or posts, and hemispherical-top pillars, the geometrical area of the plane was considered to be a rectangle (Figure 3c–d), but was considered to be a hexagon for the microbowl arrays (Figure 3b,e). Therefore, it was necessary to specify exactly the contact-angle equation for the theoretical predictions. As previously mentioned, the air-trapping mode in this geometry was dominant. In this work,

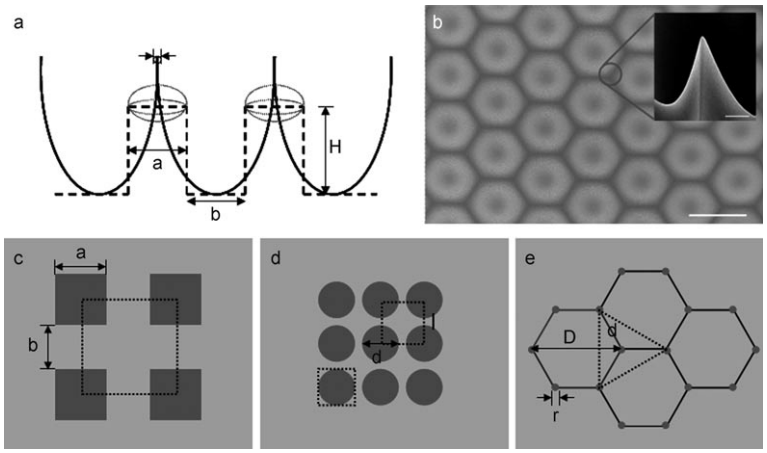

Figure 3. Model comparison of the Cassie–Baxter microbowl array with previously reported arrays. a) Comparison of cross-sectional views of square pillars (dashed line), cylindrical asperities, or posts and hemispherical-top pillars (round dot, gray line), and the Cassie–Baxter microbowl array (solid line). b) Top view of an SEM image of the Cassie–Baxter microbowl array. The scale bar is 20 μm. The inset shows the projected peak and the scale bar is 2 μm. c) Bird's-eye-view sketch of the square pillars. d) Bird's-eye-view sketch of the cylindrical asperities or posts and hemispherical-top pillars. e) Bird's-eye-view sketch of the Cassie–Baxter microbowl array.

we assumed that the trapped air in the microbowl was elastic and, therefore, Hooke's Law was valid for the deduction of the roughness factor and area fraction. Meanwhile, considering the lower surface energy after silanization, it was assumed that the elastic force was superior to the surface friction. The basic Young equation for determining the equilibrium shape of a liquid drop on a surface, $\gamma_{SV} - \gamma_{SL} = \gamma_{LV}\cos\theta$, was considered here, where γ_{SV}, γ_{SL}, and γ_{LV} denote the surface tensions of solid–vapor, solid–liquid, and liquid–vapor interfaces, respectively. Therefore, in this work, the roughness factor r_f and area fraction f were given by (see Supporting Information)

$$f = \frac{\pi r^2}{\frac{3\sqrt{3}}{4}d^2} \approx \frac{\pi}{3\sqrt{3}}b^2\left(\frac{d}{h}\right)^{8/3} = A\left(\frac{d}{h}\right)^{8/3} \quad (1)$$

$$r_f = \frac{\pi r\sqrt{r^2+l^2}}{\frac{3\sqrt{3}}{4}d^2} + 1 \approx A\frac{d^{5/3}}{h^{8/3}}\sqrt{(d^2+4h^2)} + 1$$
$$= A\left(\frac{d}{h}\right)^{5/3}\sqrt{\left(\left(\frac{d}{h}\right)^2+4\right)} + 1 \quad (2)$$

At equilibrium, we applied the Cassie–Baxter formula to get the expression for the apparent contact angle

$$\cos\theta_{app} = r_f f\cos\theta_\gamma + f - 1$$
$$= A^2\frac{d^{13/3}}{h^{16/3}}\left(\sqrt{d^2+4h^2}\right)\cos\theta_\gamma + A\left(\frac{d}{h}\right)^{8/3}(\cos\theta_\gamma + 1) - 1$$
$$= A^2\left(\frac{d}{h}\right)^{13/3}\left(\sqrt{\left(\frac{d}{h}\right)^2+4}\right)\cos\theta_\gamma + A\left(\frac{d}{h}\right)^{8/3}(\cos\theta_\gamma + 1) - 1 \quad (3)$$

where b is 0.63, A is a constant ($b^2\pi/3\sqrt{3}$), and d and h are the radius and height of the microbowl, respectively. θ_{app}, as expected, is dependent on the geometric parameters (d/h) at the critical point. In qualitative terms, according to Equation (3), to ensure superhydrophobicity, $\cos\theta_{app}$ should be as close to -1 as possible. This was ensured by using the smallest possible value of d/h available for the fabrication process. This is in agreement with previously reported results that stated that a forest of nanopillars with appropriate spacing would be an excellent superhydrophobic surface.[12,13] In the following sections, we report the experimental verification of the effect of the two crucial geometric parameters, d and h, on the apparent contact angle of a given microbowl array surface.

From two representative SEM images of the geometric surface (Figure 4a–b), a perfectly ordered and periodic microbowl array with different heights was observed. The bowl-like shape (the overall shape resembled neolithic pottery with a smooth interior surface) and the wall notches were clearly visible. The wall notches between the bowls were the result of interference among adjacent microbowls during UV exposure that was dependent on the height and diameter. This phenomenon is also observed in other dimensions (Figures 5a–c and 6a–c). The radius of the sharp apex of the microbowl was measured on the nanoscale. Five kinds of microbowl-arrayed surfaces with different dimensions were fabricated to verify our theoretical predictions. We found height-dependent hydrophobicity (Figure 4c); the apparent contact angle noticeably increased with increasing height and the surface changed from moderately hydrophobic (always the case with water, where contact angles never exceed the typical 120°)[4] to a superhydrophobic state. Additionally, there was no obvious variation, even when the contact angles were measured eight times at different sites.

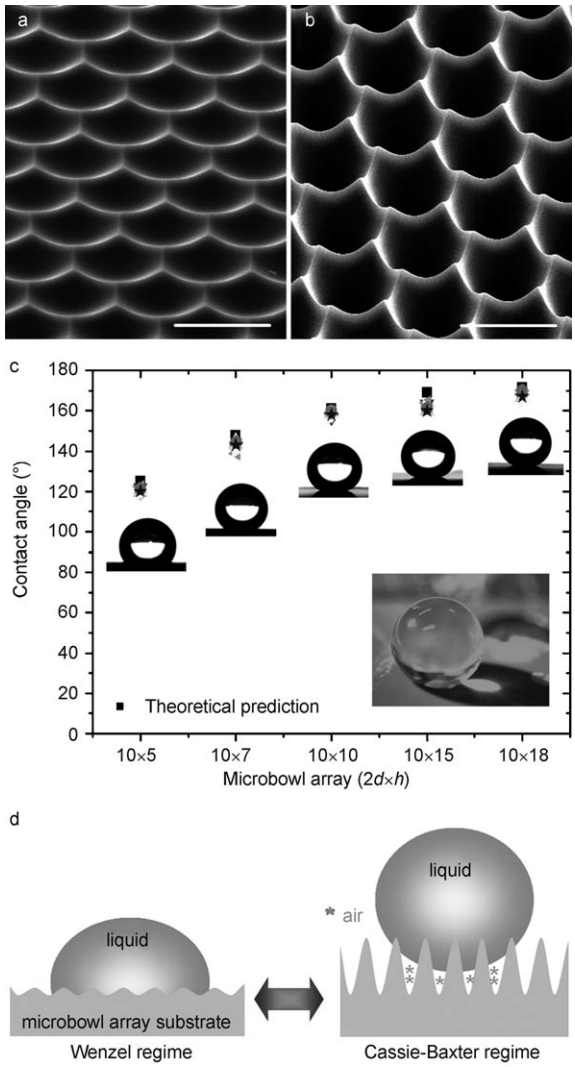

Figure 4. a, b) Typical SEM images of a different Cassie–Baxter microbowl array with a titling angle of 40° (5000×, the scale bar is 10 μm). a) 10×2, b) 10×7. c) The height-dependent hydrophobic behavior of a microbowl-arrayed surface and the corresponding theoretical prediction. The inset shows a micrographic picture of a droplet on a 10×18 microbowl array surface. d) Schematic of the possible behaviors of a droplet on different microbowl-array interfaces (height effect under the same diameter) according to the theoretical model. If the structure is too low, the droplet wets the surface and enters the Wenzel. When the height of the structure was increased, the surface is made of small protrusions, which cannot be filled by the liquid and are therefore filled with air; the wettability enters the Cassie–Baxter regime.

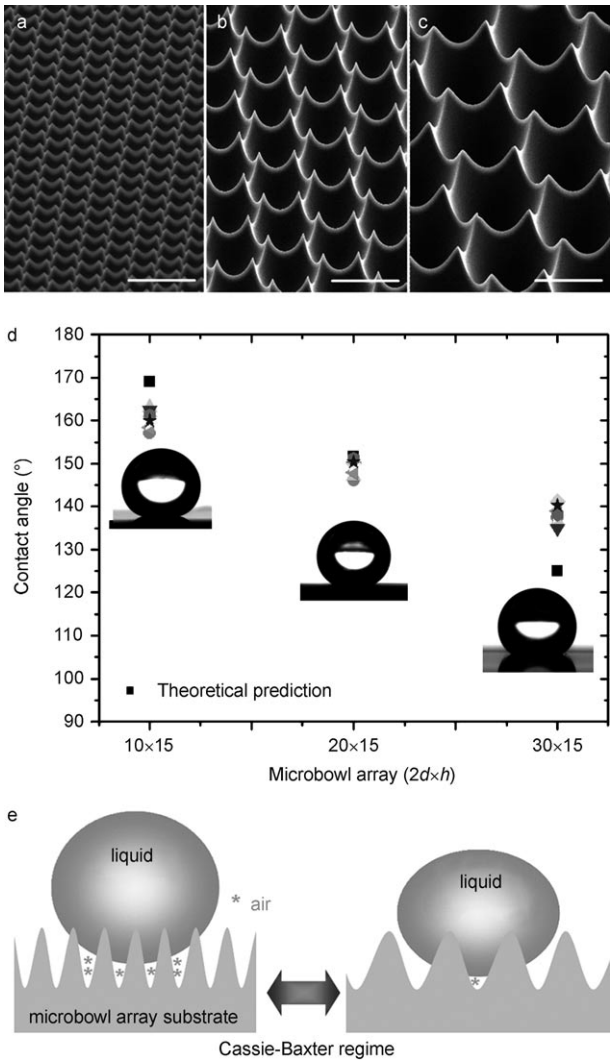

Figure 5. a–c) Typical SEM images of a different Cassie–Baxter microbowl array with a tilt angle of 40° (2000×, the scale bar is 20 μm). a) 10×15, b) 20×15, c) 30×15. d) The diameter-dependent hydrophobic behavior of a microbowl array and the corresponding theoretical prediction, e) schematic of the possible behaviors of a droplet on different microbowl-array interfaces (diameter effect under the same height) according to the theoretical model. However, if the structure is too wide, the Wenzel regime is entered.

Again, this supported the notion that the surface was extremely uniform. For a 10×18 arrayed surface, a micrographic picture showing an almost ball-shaped droplet on its surface (the inset in Figure 4c) verified that the artificially engineered microbowl surface was superhydrophobic. Comparing the five experimental results with the theoretical predictions from the analytical model for each case, we found the contact angles were very close to the predictions; the dispersion of the values was within experimental error. In addition to the direct evidence previously shown, we were also able to predict the contact-angle for other dimensions; for 10×20, 10×25, 10×30, 10×40, 10×50, 10×60, 10×100, the predicted contact angles were 172.6°, 174.6°, 175.7°, 177.1°, 177.8°, 178.3°, 179.1°, respectively. In theory, the contact angle would approach 180° as the height of the microbowls increases. A capillary effect was considered for in the case of the smallest value of d/h. This prediction strongly suggested that extremely superhydrophobic surfaces would be formed with an increasingly small value of d/h, using microfabrication techniques, according to our suggested model. This was in agreement with previous reports about the design of pillar and post microstructures.[13] Therefore, we concluded that, in these situations, height was a crucial parameter that governed the superhydrophobicity and that the increased height of microbowls prevented water from intruding into the space of the bowled structure. However, it must be noted that a larger deviation distribution was obtained for the 10×2 microbowl array surface (Figure 4) than from the proposed air-trapping model. On this substrate, a droplet was able to wet the surface, indicating that the Wenzel regime [26] was the dominant regime, as schematically shown in Figure 4d.

Figure 5 highlights the comparison between the results of hydrophobic behavior from the experimental data and those from theoretical predictions for microbowl-arrayed surfaces with different diameters. Corresponding surface morphologies for three kinds of substrates are shown in Figure 5a–c. The wall notches between the bowls are clearly observed. The trend measured for apparent contact angles revealed a diameter-dependent hydrophobic behavior, that is, the contact angle decreased as the diameter of microbowls increased (Figure 5d). As illustrated in Figure 5e, when the diameter increased, the structure widened, d/h became larger, and $\cos\theta$, in Equation 3, deviated from -1. This resulted in a decreased contact angle but the prediction for the 50×15 microbowl-arrayed surface disagreed with our data. This disagreement indicated that liquid fully saturated the depressions of the rough surface when the structure was too wide and then trapped air no longer needed to be considered. This suggested that the air-trapping model again was replaced again by the Wenzel model that is based on the hypothesis of a saturated surface.

We continued to investigate the hydrophobic behavior of microbowl array surfaces with the same diameter and height, that is, with identical aspect ratios (Figure 6d). Moreover, the surface morphology of three kinds of dimensions was studied (Figure 6a–c). In the SEM images, we found cases that differed vastly from the two aforementioned cases (Figures 4a–b and 5a–c). For a 30×30 microbowl array, the wall notches between the bowls were deeper, and the apexes of the microbowl became almost triangular pyramid pillars (Figure 6c). In addition, the sharp apexes and the wall notches were obviously different from each other (Figure 6a–c). If one had taken a glance at the surface properties according to the previous model, one could have thought that the notches and apexes contributed significantly to the superhydrophobicity. In contrast, with the model proposed, we observed that they were not important parameters for governing the antiwetting properties. The measured distribution of contact angles was almost within the experimental error (Figure 6d). Here, the force of trapped air is assumed to be equal, as shown in Figure 6e. From this result, we can ascertain that sharper apexes and deeper wallnotches had little effect on contact angles in the

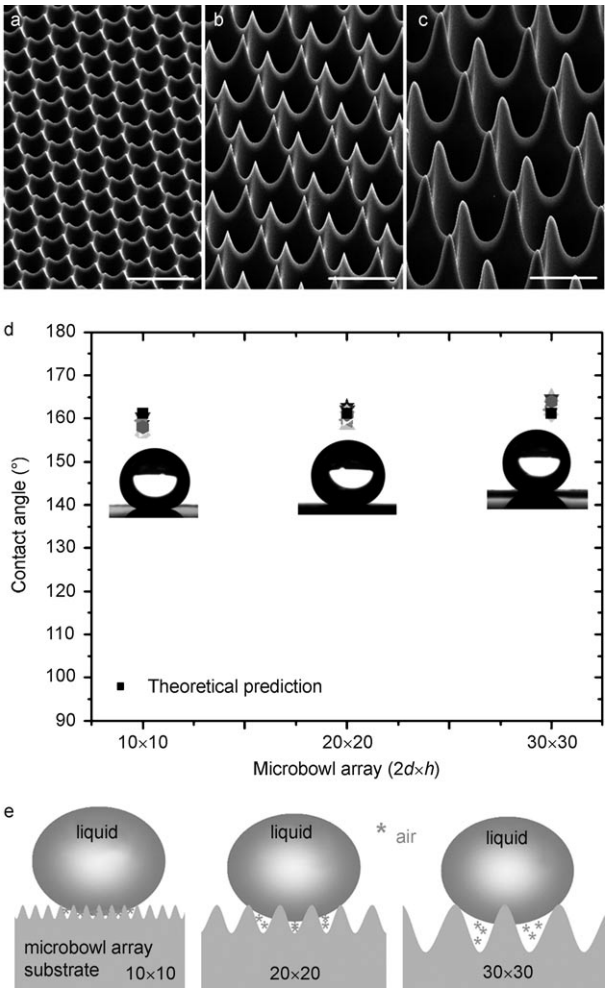

Figure 6. a–c) Typical SEM images of a different Cassie–Baxter microbowl array with a tilt angle of 40° (2000×, the scale bar is 20 μm). a) 10×10, b) 20×20, c) 30×30. d) The hydrophobic behavior of a microbowl array with the same ratio between diameter and height and the corresponding theoretical prediction. e) Schematic of the possible behaviors of a droplet on different microbowl-array interfaces according to the theoretical model.

microbowl array. We demonstrated that a too wide diameter of microbowl would result in a decreased contact angle. Furthermore, a deeper height would form a superhydrophobic surface. When these two parameters were both changed together, the suggested analytical model was able to provide a guideline to design an optimized surface morphology.

This study thus emphasized a one-step technique for the fabrication of a perfectly ordered wafer-scale microbowl array and demonstrated, both experimentally and theoretically, their size-dependent superhydrophobic behaviour. Although we have not discussed sliding angles, we observed that the water droplet could immediately roll off the sample surfaces during contact-angle measurements. This suggested a very small sliding angle because of the wafer-scale uniformity of the surface. However, more work will have to be done in order to obtain quantitative values. Finally, we believe this study can provide a guideline for the design of an appropriate surface structure to achieve desired surface-wetting properties and gave us a better understanding of the evolution and quantitative studies of highly regular superhydrophobic surfaces.

Experimental Section

Fabrication of the microbowl array: The fabrication process of a photoresist microbowl array using three-dimensional diffuser lithography,[18,19] which utilizes randomized ultraviolet (UV) light, is schematically shown in Figure 1. A circular or elliptical cross section formed in the photoresist. After spin coating with a thick AZ9260 positive photoresist (Clariant Co. Ltd.) layer at 1500 rpm for 0.5 s to achieve a thickness of 80 μm on the substrate, followed by soft-baking at 85°C for 1 h, the thick photoresist film was exposed to UV light through a diffuser and a mask. During the diffuser lithography, UV exposure at 4500 mJ cm^{-2} was performed through a sandblasted diffuser plate (F43-725; Edmund Optics Co. Ltd.). The various aspect ratios in the microbowl array were created by adjusting the flood exposure dose from 20 mJ cm^{-2} to 200 mJ cm^{-2}. Because the exposed regions of the adjacent microbowl patterns started to interfere and overlap each other with, the photoresist microbowl array was formed after development of UV exposure. The array surface was silane modified by depositing vapor-phase tridecafluoro -1,1,2,2- tetrahydrooctyltricholrosilane (CF_3-$(CF_2)_5(CH_2)_2SiCl_3$, Fluka).

Characterization: Sample morphologies were investigated using a Philips XL 30 AFEG scanning electron microscope (SEM, Eindhoven, The Netherlands). Contact angles (CA) were measured on a Dataphysics OCA20 CA system at ambient temperature. Measurements were taken eight times in different locations for each sample. The droplet volume that was used in the experiments was 12 μL.

Keywords:
lithography · microbowl arrays · one-step fabrication · superhydrophobicity · size dependence

[1] L. Feng, S. H. Li, Y. S. Li, H. J. Li, L. J. Zhang, J. Zhai, Y. L. Song, B. Q. Liu, L. Jiang, D. B. Zhu, *Adv. Mater.* **2002**, *14*, 1857–1860.
[2] X. J. Feng, L. Jiang, *Adv. Mater.* **2006**, *18*, 3063–3078.
[3] H. Y. Erbil, A. L. Demirel, Y. Avci, O. Mert, *Science* **2003**, *299*, 1377–1380.
[4] A. Lafuma, D. Quéré, *Nat. Mater.* **2003**, *2*, 457–460.
[5] T. Onda, S. Shibuichi, N. Satoh, K. Tsujii, *Langmuir* **1996**, *12*, 2125–2127.
[6] J. Bico, C. Marzolin, D. Quéré, *Europhys. Lett.* **1999**, *47*, 220–226.
[7] Z. Yoshimitsu, A. Nakajima, T. Watanabe, K. Hashimoto, *Langmuir* **2002**, *18*, 5818–5822.
[8] D. Öner, T. McCarthy, *Langmuir* **2000**, *16*, 7777–7782.
[9] R. Blossey, *Nat. Mater.* **2003**, *2*, 301–306.
[10] E. Martines, K. Seunarine, H. Morgan, N. Gadegaard, C. D. W. Wilkinson, M. O. Riehle, *Nano Lett.* **2005**, *5*, 2097–2103.
[11] E. Martines, K. Seunarine, H. Morgan, N. Gadegaard, C. D. W. Wilkinson, M. O. Riehle, *Langmuir* **2006**, *22*, 11230–11233.

[12] B. He, N. A. Patankar, J. H. Lee, *Langmuir* **2003**, *19*, 4999–5003.
[13] N. A. Patankar, *Langmuir* **2003**, *19*, 1249–1253.
[14] C. Dorrer, J. Rühe, *Langmuir* **2007**, *23*, 3820–3824.
[15] M. Lundgren, N. L. Allan, T. Cosgrove, *Langmuir* **2007**, *23*, 1187–1194.
[16] L. B. Zhu, Y. H. Xiu, J. W. Xu, P. A. Tamirisa, D. W. Hess, C. P. Wong, *Langmuir* **2005**, *21*, 11208–11212.
[17] X. F. Gao, X. Yan, X. Yao, L. Xu, K. Zhang, J. H. Zhang, B. Yang, L. Jiang, *Adv. Mater.* **2007**, *19*, 2213–2217.
[18] S. I. Chang, J. B. Yoon, H. Kim, J. J. Kim, B. K. Lee, D. H. Shin, *Opt. Lett.* **2006**, *31*, 3016–3018.
[19] S. I. Chang, J. B. Yoon, *Opt. Express* **2004**, *12*, 6366–6371.
[20] X. F. Gao, X. Yao, L. Jiang, *Langmuir* **2007**, *23*, 4886–4891.
[21] J. Genzer, K. Efimenko, *Biofouling* **2006**, *22*, 339–360.
[22] J. Genzer, K. Efimenko, *Science* **2000**, *290*, 2130–2133.
[23] D. Quéré, *Physica A* **2002**, *313*, 32–46.
[24] G. McHale, N. J. Shirtcliffe, S. Aqil, C. C. Perry, M. I. Newton, *Phys. Rev. Lett.* **2004**, *93*, 036 102–036 104.
[25] A. B. D. Cassie, S. Baxter, *Trans. Faraday Soc.* **1944**, *40*, 546–551.
[26] R. N. Wenzel, *Ind. Eng. Chem.* **1936**, *283*, 988–994.

Received: September 22, 2007
Published online on January 17, 2008

